Arsenic-bridged magnetic interactions in an emerging two-dimensional FeAs nanostructure on MnAs

Christian Helman,[1,2,*] Valeria Ferrari,[3,4] and Ana Maria Llois[3,4,5]

[1]*Gerencia de Tecnologías de la Información y las Comunicaciones, Centro Atómico Constituyentes, (1650) San Martín, Argentina*

[2]*Instituto Sabato, Universidad Nacional de San Martín, (1650) San Martín, Argentina*

[3]*Gerencia de Investigación y Aplicaciones, Centro Atómico Constituyentes, (1650) San Martín, Argentina*

[4]*Consejo Nacional de Investigaciones Científicas y Técnicas, (C1033AAJ) Buenos Aires, Argentina*

[5]*Departamento de Física Juan José Giambiagi, FCEN, Universidad de Buenos Aires, (1428) Buenos Aires, Argentina*

(Received 19 January 2015; published 13 August 2015)

The extreme case of an Fe monolayer deposited onto a manganese arsenide (MnAs) substrate is analyzed using density functional theory. We find that an FeAs quasi-two-dimensional antiferromagnetic surface nanostructure emerges. This nanostructure, which is magnetically nearly decoupled from the substrate, is due to bonding effects arising from the arsenic atoms bridging the Fe magnetic interactions. These interactions are studied and modeled using a Heisenberg-type Hamiltonian. They display an angular dependence which is characteristic of superexchange-like interactions, which are of the same order of magnitude as those appearing in Fe-based pnictides.

DOI: 10.1103/PhysRevB.92.075416 PACS number(s): 75.70.Ak, 75.30.Et, 75.10.Hk

I. INTRODUCTION

In the last decade, due to the technological importance of the realm of spintronic devices, there has been theoretical and experimental interest in the study of Fe films grown on metallic [1,2] and semiconducting substrates [3,4]. Among the metallic substrates of interest, work has been done on Fe monolayers grown on tungsten [5] and iridium [6], and recently, much effort has been devoted to the properties of nanometer-thick Fe epilayers epitaxially grown on MnAs/GaAs(001) [7–10].

MnAs is a magnetic metallic material with several polymorphic transformations as a function of temperature [11–13]. Interestingly, at low temperatures, when MnAs is in its ferromagnetic α phase, it has been observed that deposited Fe films are magnetically decoupled from the MnAs substrate [7,8]. This has led to the idea of taking advantage of the magnetic and structural phase transition of MnAs, which happens near room temperature, and using it to develop a magnetic template [7,14,15].

Recent works [15,16] studying ultrathin Fe films grown on MnAs/GaAs(001) substrates proposed and experimentally explored a possible application of these combined systems. The authors made use of a laser to locally induce an Fe magnetization switching, benefiting from the temperature-driven phase transition of MnAs [16].

Actually, the involved magnetic interactions at the interesting Fe/MnAs interface still remain an open question [16]. The purpose of the present work is therefore to study the magnetic interactions at the early stage of Fe deposition on MnAs by analyzing the extreme case of an Fe monolayer (ML). This Fe coverage limit has not yet been approached either theoretically or experimentally, and we expect that our findings will open the way to further explore it. We consider that the MnAs substrate is in its α phase, which is the stable structure below room temperature.

We find that a two-dimensional (2D) FeAs nanostructure forms at the surface under study. This happens if one considers the experimental growth conditions of the MnAs substrate, which involve an As-rich atmosphere rendering an As termination [17]. By means of a Heisenberg-type Hamiltonian, we show that the magnetic couplings at this nanostructure and at the interface can be explained through a mediation mechanism led by the As atoms. The surface nanostructure displays a magnetic ground state completely different from the one of a thicker Fe overlayer [18]. It is likely that the emerging physics at this early growth stage presents some kind of similarity to the one of FeAs-based materials, which have been widely studied in the last few years [19–21].

II. CALCULATION DETAILS

We simulate the α-MnAs substrate with a supercell built by three MnAs unit cells separated by a vacuum region of 10 Å [22]. The periodic slab electronic calculations are performed within the framework of *ab initio* density functional theory (DFT) as implemented in the VASP code [23]. Projector augmented-wave pseudopotentials are used [24], along with the generalized gradient approximation to the exchange and correlation potential within the Perdew-Burke-Ernzerhof parametrization [25]. The kinetic energy cutoff is set to 350 eV while a $20 \times 20 \times 1$ mesh in the reciprocal space is considered. Internal atomic coordinates are fully relaxed until forces are smaller than 0.04 eV/Å.

We assume that α-MnAs grows in the $[1\bar{1}00]$ direction; therefore, the in-plane cell parameters of the slab are taken as $a = 3.73$Å and $b = 5.69$Å [22]. No inversion symmetry is imposed in order to have full MnAs formula units in the unit cell of the periodic slab, and consequently, the two free surfaces of the slab show different atomic terminations, thus allowing us to analyze the two possible interfaces between the Fe film and the MnAs substrate.

*helman@tandar.cnea.gov.ar

III. INTERPLAY BETWEEN CRYSTAL STRUCTURE AND MAGNETISM

We focus on the situation given by the experimental growth conditions of MnAs, which favor the As termination on top of which the Fe ML is assumed to be deposited [17]. Fe impurities in MnAs bulk occupy preferentially Mn-substitutional positions [26,27], and therefore, we propose that the interfacial Fe atoms follow the MnAs structure occupying Mn sites. After relaxation of the atomic coordinates, a sharp interface without any Fe interdiffusion is obtained, but an important reconstruction involving the As atoms occurs. The As-terminated surface presents two nonequivalent atomic positions for the As atoms. One of the arsenic nonequivalent positions, denoted by As_{low}, lies slightly above the last Mn plane of the substrate, while the other one, labeled As_{top}, ends up lying, after relaxation, close to the Fe plane, rendering a quasi-2D nanostructure, as shown in Fig. 1(a). It is worthwhile to remark that our calculations indicate that the Fe monolayer is stable for both terminations of the MnAs substrate.

Taking into account that crystal structure and magnetism influence each other, we propose different magnetic configurations (MCs) for the 2D nanostructure, allowing the internal positions within the cell to relax in each case. In Table I, all the considered MCs are summarized along with the resulting Fe magnetic moments and the relative energies of the configurations. For different MCs, positive and negative Fe magnetic moments respectively imply parallel and antiparallel alignment with respect to the Mn atoms of the substrate. These moments are denoted by ↑ and ↓ in Table I, respectively. Note that the magnetic moments of the Fe atoms are close to their Fe bulk value ($\approx 2.22\mu_B$) despite being in a 2D nanostructure.

Figure 1 shows the relaxed atomic structure and a schematic top view of the magnetic ground state denoted as AFM-1. To characterize AFM-1, we present in Fig. 2 the charge- and spin-density distributions for different planes of the slab. It can be observed that beyond the uppermost As layer, the electronic distribution of the substrate is barely affected by the presence of the Fe overlayer. Figures 2(a) and 2(c) show that Fe and As atoms are covalently bonded, and this covalency is noticeably stronger than the one between Mn and As atoms. The topmost Mn layer relaxes slightly towards the developed Fe-As overlayer, and the only appreciable effect on the Mn atoms is a small deformation of the spin cloud due to the antiferromagnetic (AFM) character of the Fe network [see Fig. 2(b)].

TABLE I. Energy differences among the magnetic configurations (MC) considered. In the second column, the magnetic configurations are labeled with the spin orientation corresponding to the Fe atoms numbered in Fig. 1(a) following the order $|\mathbf{1234}\rangle$. All the energies ΔE are referred to the AFM-1 ground-state configuration. The Fe-magnetic moments (MM) are also given.

MC	$\|\mathbf{1234}\rangle$	ΔE (meV/Fe ion)	MM(↑) (units of μ_B)	MM(↓) (units of μ_B)
AFM-1	$\|\uparrow\downarrow\downarrow\uparrow\rangle$	0.0	2.27	−2.29
AFM-2	$\|\downarrow\uparrow\downarrow\uparrow\rangle$	48.1	2.22	−2.15
AP	$\|\downarrow\downarrow\downarrow\downarrow\rangle$	78.8		−2.20
P	$\|\uparrow\uparrow\uparrow\uparrow\rangle$	101.4	2.12	
AFM-3	$\|\uparrow\uparrow\downarrow\downarrow\rangle$	102.3	2.10	−2.25

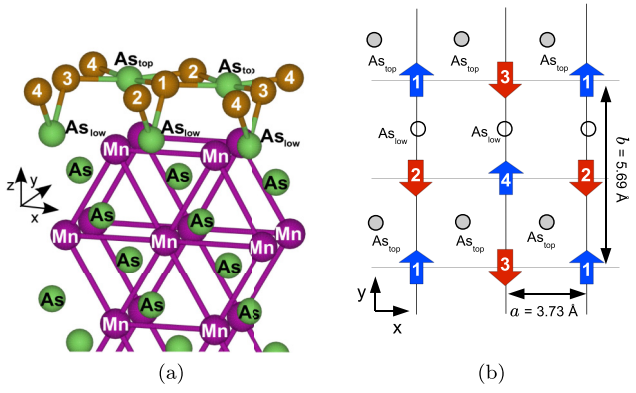

FIG. 1. (Color online) (a) Relaxed structure of an Fe monolayer on the MnAs substrate. Green, violet, and brown spheres stand for As, Mn, and Fe ions, respectively. There are two types of As atoms at the interface, namely, As_{top} (lying in the Fe plane) and As_{low} (located in between the Fe and Mn planes). The topmost 2D nanostructure is composed of Fe and As_{top} atoms. (b) Schematic top view of the FeAs nanostructure displaying the ground-state antiferromagnetic configuration (AFM-1). As_{low} atoms are shown for reference. The up (down) arrows denote parallel (antiparallel) Fe magnetic moments with respect to the Mn ones. The numbers within the arrows refer to Fe atoms as in (a).

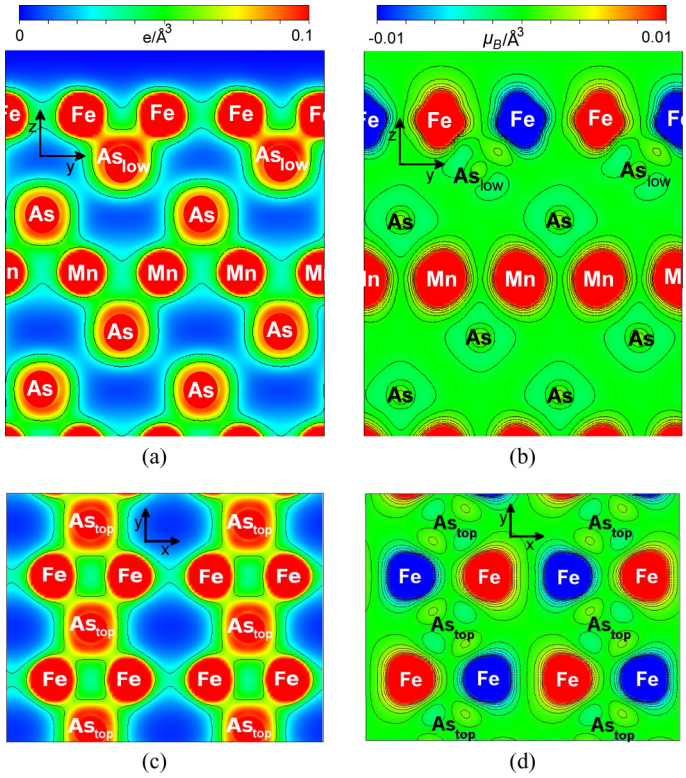

FIG. 2. (Color online) (left) Charge and (right) spin density maps. (a) and (b) The zy cut containing As_{low} atoms. (c) and (d) The xy cut containing the FeAs nanostructure. See labels and coordinate system in Fig. 1.

The spin densities shown in Figs. 2(b) and 2(d) reveal a strong localization of the Fe atoms' magnetic moments. The magnetic role played by the bridging As atoms can be recognized in the reconstructed surface layer. Although As_{low} presents a small net magnetization ($<0.01\mu_B$), its lobes are antiferromagnetically aligned with the nearest Fe atoms.

The above-described features point towards the presence of a superexchange-like mechanism as the main contribution to the magnetic interactions among the Fe atoms at the nanostructure [19].

Actually, the magnetic interaction is highly dependent on the bonding distance, namely, the Fe-As interactions within the nanostructure. To highlight this issue, we perform a simulation where the Fe atoms are rigidly moved away from the substrate. Figure 3(a) shows that the AFM-1 configuration is the lowest-energy one for separations Δd of up to 0.5% of the equilibrium distance. For displacements beyond these values, the P and AP arrangements are the energetically preferred ones and are nearly degenerate. As denoted in Table I, P and AP configurations have the Fe spins aligned among them while being parallel and antiparallel aligned to the Mn atoms of the substrate, respectively. Therefore, the degeneracy of P and AP configurations indicates a small coupling between the Fe overlayer and the MnAs substrate for those displacements for which the As bridging breaks down. Otherwise, in another simulation, the nanostructure as a whole (that is, the Fe overlayer along with the As_{top} atoms) is rigidly separated from the substrate. The results are displayed in Fig. 3(b). In this case, the AFM-1 configuration is always the preferred one, independent of the value of Δd, and no degeneracy between P and AP is observed.

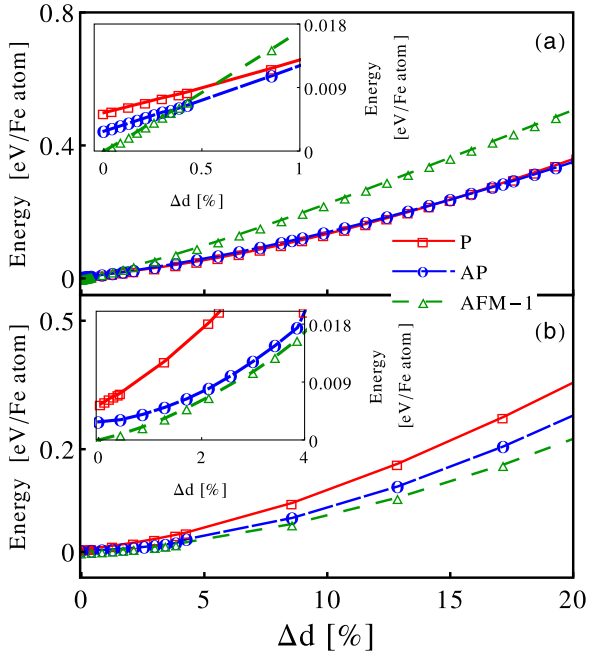

FIG. 3. (Color online) Energy behavior of different magnetic configurations when (a) an Fe-only layer is rigidly separated from the substrate or (b) the Fe-As_{top} layer (i.e., nanostructure) is separated from the substrate. Δd gives the relative displacement with respect to the equilibrium distance for each magnetic configuration. Both insets are zoomed-in areas of the corresponding graphs. The green dashed line is the energy evolution of AFM-1, and dashed blue and solid red lines correspond to the AP and P configurations, respectively. The inset in (a) shows that for small separations from the equilibrium position, the AFM-1 configuration is no longer the ground state. On the contrary, when Fe and As_{top} atoms move rigidly together as in (b), AFM-1 is always the ground state.

We conclude that the antiferromagnetic configuration AFM-1 is the lowest-energy one and is originated by the presence of the As_{top} atoms. This behavior of the Fe monolayer is similar to what has already been reported for a monolayer of Fe grown on W(001), which at the equilibrium interlayer distance shows an AFM ground state [2]. As in our case it is the hybridization with the substrate that dominates the Fe-Fe magnetic interaction. Additionally, the slight preference for the AP configuration over the P one in Fig. 3(b) indicates a weak antiferromagnetic coupling between the FeAs nanostructure and the closest Mn layer. This weak interaction reveals the decoupling role played by the As_{low} atoms in the determination of the magnetic interactions among Fe and Mn.

IV. MODELING THE MAGNETIC COUPLINGS

The magnetic ground state of the emerging surface nanostructure is similar to the ones found in the iron pnictides [19–21]. In previous works [19,20,28] on iron pnictides, it was proposed that the Fe-Fe interactions are modified by As mediation and that they depend on the angle formed by the different Fe-As bonds appearing in the structures. Actually, in these interactions all valence orbitals of the different atoms are involved, and it is difficult to isolate the orbitals responsible for each Fe-Fe or Fe-Mn coupling [28]. Therefore, following what was done in Ref. [19], we consider average As-bridged interactions among atomic spin moments to model the magnetic couplings of the system. Direct Fe-Fe interactions are also taken into account.

In order to estimate the values of the couplings, we use the atomic moment approximation with collinear configurations. Total energies obtained for different MCs within DFT are mapped onto a Heisenberg-type Hamiltonian. This Hamiltonian can be separated into two terms, $\hat{\mathbf{H}}_0$, which is independent of any MC configuration, and a second contribution that depends on spin operators $\hat{\mathbf{S}}$ and magnetic couplings J_{ij}. The spin operators are replaced by $\sqrt{s(s+1)}\,\sigma_i$, where σ_i can take the values $+1(\uparrow)$ or $-1(\downarrow)$, denoting the magnetic moment orientation at site i. The proposed Hamiltonian is then given by

$$H = \hat{\mathbf{H}}_0 - \sum_{i \neq j} J_{ij}(\sigma_i \cdot \sigma_j). \tag{1}$$

The values of the respective magnetic moments are included in the definition of J_{ij}, which can be positive or negative, denoting ferromagnetic or antiferromagnetic interactions.

As a whole, we consider seven different J_{ij} exchange parameters labeled as follows: J_1 to J_4 indicate Fe-Fe interactions mediated by an As atom for four different Fe-As-Fe angles, denoted α. J_5 denotes a direct Fe-Fe interaction, while J_6 and J_7 stand for Fe-Mn couplings mediated by As for different Fe-As-Mn angles, denoted β. J_6 (J_7) represents an average Fe-Mn interaction for β larger (smaller) than 90°.

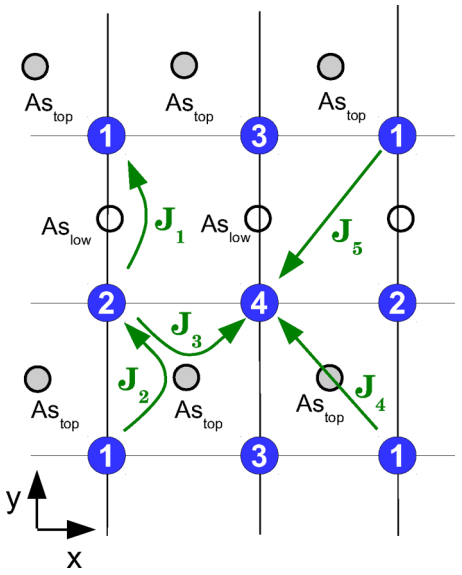

FIG. 4. (Color online) Schematic of the magnetic couplings proposed within a Heisenberg model for the FeAs nanostructure that develops when an Fe monolayer is deposited on As-terminated MnAs. The blue circles represent Fe atoms, with numbers corresponding to those in Fig. 1(a). The model considers four different magnetic arsenic-mediated Fe-Fe magnetic interactions, J_1 to J_4, sustaining different angles and a long-range Fe-Fe direct interaction, J_5. The Fe-Mn couplings (J_6 and J_7) are also considered in our model but are not shown in this picture.

The couplings among the Fe atoms of the nanostructure are schematically depicted in Fig. 4. The values of the different J_i are obtained through a least-squares fitting procedure[29] over ten different MCs, namely, eight AFM arrangements and also the AP and P configurations.

The resulting magnetic couplings, given in Table II , reveal an interesting angular dependence. In the case of the As-bridged Fe-Fe interactions, the magnetic coupling is increasingly antiferromagnetic in the angular range $73^\circ < \alpha < 106^\circ$ (J_{1-3}), while for $\alpha \approx 180^\circ$ (J_4) the coupling is ferromagnetic. The As-mediated Fe-Mn interactions are antiferromagnetic for $\beta < 90^\circ$ and ferromagnetic otherwise (J_6 and J_7).

We try to understand the above angular dependence by means of Goodenough's rules [30] by isolating the three atoms involved in each As-bridged interaction. For this purpose, Fe-As-Fe and Fe-As-Mn triatomic structures are considered.

TABLE II. Magnetic spin couplings corresponding to the interactions depicted in Fig. 4. Here α is the Fe-As-Fe angle, and β is the Fe-As-Mn one.

Label	Mediator	Atoms	Angle	Distance (Å)	J(meV/atom)
J_1	As_{low}	$\widehat{1,2}$	$\alpha = 73^\circ$	2.89	−21.2
J_2	As_{top}	$\widehat{1,2}$	$\alpha = 79^\circ$	2.8	−31.5
J_3	As_{top}	$\widehat{1,3}$	$\alpha = 106^\circ$	3.73	−36.7
J_4	As_{top}	$\widehat{1,4}$	$\alpha = 180^\circ$	4.66	4.4
J_5	direct			4.72	−4.3
$J_6^{Fe,Mn}$	both As atoms		$\beta > 90^\circ$		−6.7
$J_7^{Fe,Mn}$	both As atoms		$\beta < 90^\circ$		3.1

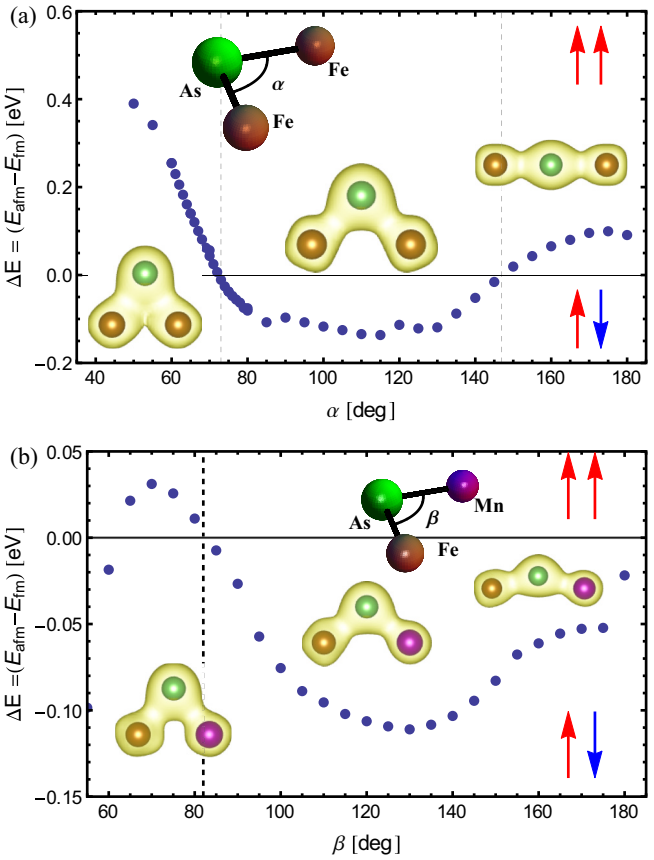

FIG. 5. (Color online) Energy difference between antiferromagnetic and ferromagnetic configurations for simulated (a) Fe-As-Fe and (b) Fe-As-Mn structures as a function of the corresponding angle, α or β. Positive (negative) values indicate ferromagnetic (antiferromagnetic) coupling. In (a) two magnetic transitions are observed when α increases, one from ferromagnetic to antiferromagnetic at 72° and the reverse at 150°. In (b) there is only one transition at 85°. A typical charge isosurface graph is superimposed at each stage.

We perform simulations in which the angles α and β held by these structures are changed while the As-Fe and As-Mn distances to the values they attain after relaxation in the Fe/MnAs heterostructure are kept fixed. Within this structure, both FM and AFM alignments are proposed. In Figs. 5(a) and 5(b), the energy differences between AFM and FM configurations as a function of angles α and β are shown.

The Fe-As-Fe triatomic structure presents two magnetic transitions, one at 72° when the magnetic ground state changes from FM to AFM and the other one at 150° when the magnetic state turns FM again. Prior to the first transition, the FM alignment is actually due to a direct interaction between the two Fe atoms because their distance is less than the nearest-neighbor distance in bulk Fe. In this small-angle region, the charge isosurface shown in Fig. 5(a) reveals this direct Fe-Fe interaction. Increasing the angle α, the Fe-Fe coupling starts being mediated by As, and the triatomic structure turns AFM. As can be seen in Fig. 5(a), between 72° and 150° the lowest-energy configuration is antiferromagnetic. According to Goodenough's rules, this is due to the fact that the As p_π

orbital hybridizes with the Fe d_{yz} and Fe d_{xz} ones, while the As p_σ orbital mainly hybridizes with Fe $d_{x^2-y^2}$.

In the extreme limit case of 180°, the interacting As orbitals are mainly the p_z and p_y ones, while the bonding direction is along the $\hat{x}$ axis. These two orbitals are degenerate, hybridize with the Fe d_{xz} and Fe d_{xy} ones, and are perpendicular to the plane of the Fe-As-Fe structure. The magnetic interaction mediated by these orbitals is, in fact, FM and can also be understood with Goodenough's rules. For α between 140° and 180°, there is a competition between the AFM and the FM contributions, which gradually change their relative weight until the maximum ferromagnetic contribution is attained at 180°.

In Fig. 5(b) we focus on the Fe-As-Mn triatomic system. In this case only one magnetic transition, from ferromagnetic (FM) to AFM, is observed at $\beta = 90°$. The antiferromagnetic coupling has the same origin as the one present in the Fe-As-Fe structure discussed above. The net coupling between the nanostructure and the substrate is small compared to the net antiferromagnetic interactions within the nanostructure, pointing towards a nearly magnetically decoupled overlayer.

Going back to the 2D nanostructure, the bonding angles related to $J_1 - J_3$, which are antiferromagnetic, fall within the antiferromagnetic angular range obtained for the Fe-As-Fe structure, while the angle associated with the ferromagnetic J_4 coupling lies in the ferromagnetic angular range of the Fe-As-Fe one. For the As-mediated couplings between Mn and Fe atoms in the nanostructure, the behavior of the signs of $J_6(\beta > 90)$ and $J_7(\beta < 90)$ is also consistent with the antiferromagnetic/ferromagnetic trends obtained for the triatomic Fe-As-Mn structure in the corresponding angular range.

The fact that the results for the triatomic structures correlate so well with the parametrized Heisenberg Hamiltonian points towards a short-range-interaction scenario.

Taking the above into account, the As-bridged interatomic magnetic interactions, which define the magnetic ground state of the 2D metallic nanostructure, can be traced back to superexchange-like interactions within triatomic units.

V. FINAL REMARKS

In this work we have analyzed the reconstruction and magnetic interactions that are expected to take place after deposition of Fe on a MnAs thin film grown on GaAs(001) at the early growth stage in the Fe monolayer range. In this limit, an antiferromagnetic surface nanostructure composed of Fe and As atoms emerges in such a way that Fe-Fe magnetic interactions are mainly arsenic mediated, building Fe-As-Fe bridges. The magnetic structure of this overlayer could, in principle, be observed using spin-polarized tunneling microscopy [2]. It is interesting to remark that the As atoms at the interface provide simultaneously the magnetic interaction among Fe atoms and a mechanism decoupling the overlayer from the MnAs substrate. The magnetic interaction with the substrate is weak compared to the in-plane ones. The net exchange coupling among the interface Fe and Mn atoms, around 3.8 meV (100 Oe), is within the range expected for the effective exchange field H_{ex}, as given in Ref. [9].

Through the mapping of *ab initio* total energy results onto a Heisenberg-type Hamiltonian, we are able to characterize the As-mediated Fe-Fe magnetic interactions. The As bridge plays a crucial role in the determination of the magnetic ground state of the resulting heterostructure, in a way similar to what happens in the Fe pnictide superconductors [19]. Most of the couplings obtained for the mediated Fe-Fe interactions are of the same order of magnitude as those of the mentioned iron pnictides, that is, around 50 meV [19]. In the present case, we also consider Fe-Fe direct interactions, which are one order of magnitude smaller than the As-mediated one and similar to the As-mediated Fe-Mn interactions across the interface. The sign of these superexchange-like magnetic couplings is interpreted using triatomic Fe-As-Fe and Fe-As-Mn structures where Goodenough's rules are easily identified.

The 2D FeAs nanostructure that appears presents similarities to the FeSe monolayer recently grown on $SrTiO_3$ [4]. Therefore, our emerging system could be superconducting upon proper doping or treatment. A thorough analysis of this possibility is out of the scope of this paper.

To sum up, when depositing Fe on MnAs, at the early monolayer stage of growth, an FeAs antiferromagnetic surface nanostructure develops, which is magnetically nearly decoupled from the MnAs substrate and constitutes a 2D object that poses challenges and opportunities for heterostructure-based interface engineering.

ACKNOWLEDGMENTS

We thank L. Steren, M. Marangolo, J. Milano, and V. Vildosola for helpful discussions. C.H., V.F., and A.M.L. are supported by the Institute of Nanoscience and Nanotechnology (INN) of the Atomic Energy Agency (CNEA), Argentina, and to LIFAN (Laboratorio Internacional Franco-Argentino en Nanociencias). They acknowledge financial support from ANPCyT (PICT-2011-1187 and 1857), CONICET (PIP00273 and PIP0069CO), and UBA (UBACYT-W354).

[1] B. Hardrat, A. Al-Zubi, P. Ferriani, S. Blügel, G. Bihlmayer, and S. Heinze, Phys. Rev. B **79**, 094411 (2009).

[2] A. Kubetzka, P. Ferriani, M. Bode, S. Heinze, G. Bihlmayer, K. von Bergmann, O. Pietzsch, S. Blügel, and R. Wiesendanger, Phys. Rev. Lett. **94**, 087204 (2005).

[3] S. Mirbt, B. Sanyal, C. Isheden, and B. Johansson, Phys. Rev. B **67**, 155421 (2003).

[4] Sun Yi, Zhang Wenhao, Xing Ying, Li Fangsen, Zhao Yanfei, Xia Zhengcai, Wang Lili, Ma Xucun, Xue Qi-Kun, and Wang Jian, Sci. Rep. **4**, 6040 (2014); Ge Jian-Feng, Liu Zhi-Long, Liu Canhua, Gao Chun-Lei, Qian Dong, Xue Qi-Kun, Liu Ying, and Jia Jin-Feng, Nat. Mater. **14**, 285 (2015).

[5] B. A. Hamad and M. Richter, Phys. Rev. B **83**, 245135 (2011).

[6] Z. Tian, D. Sander, and J. Kirschner, Phys. Rev. B **79**, 024432 (2009).
[7] R. Breitwieser, M. Marangolo, J. Luning, N. Jaouen, L. Joly, M. Eddrief, V. H. Etgens, and M. Sacchi, Appl. Phys. Lett. **93**, 122508 (2008).
[8] C. Helman, J. Milano, S. Tacchi, M. Madami, G. Carlotti, G. Gubbiotti, G. Alejandro, M. Marangolo, D. Demaille, V. H. Etgens, and M. G. Pini, Phys. Rev. B **82**, 094423 (2010).
[9] M. Sacchi, M. Marangolo, C. Spezzani, L. Coelho, R. Breitwieser, J. Milano, and V. H. Etgens, Phys. Rev. B **77**, 165317 (2008).
[10] S. Tacchi, M. Madami, G. Carlotti, G. Gubbiotti, M. Marangolo, J. Milano, R. Breitwieser, V. H. Etgens, R. L. Stamps, and M. G. Pini, Phys. Rev. B **80**, 155427 (2009).
[11] N. Mattoso, M. Eddrief, J. Varalda, A. Ouerghi, D. Demaille, V. H. Etgens, and Y. Garreau, Phys. Rev. B **70**, 115324 (2004).
[12] A. K. Das, C. Pampuch, A. Ney, T. Hesjedal, L. Däweritz, R. Koch, and K. H. Ploog, Phys. Rev. Lett. **91**, 087203 (2003).
[13] L. B. Steren, J. Milano, V. Garcia, M. Marangolo, M. Eddrief, and V. H. Etgens, Phys. Rev. B **74**, 144402 (2006).
[14] M. Sacchi, M. Marangolo, C. Spezzani, R. Breitwieser, H. Popescu, R. Dealaunay, B. Rache Salles, M. Eddrief, and V. H. Etgens, Phys. Rev. B **81**, 220401 (2010).
[15] C. Spezzani, F. Vidal, R. Delaunay, M. Eddrief, M. Marangolo, V. H. Etgens, H. Popescu, and M. Sacchi, Sci. Rep. **5**, 8120 (2015).
[16] C. Spezzani *et al.*, Phys. Rev. Lett. **113**, 247202 (2014).
[17] R. Breitwieser, F. Vidal, I. L. Graff, M. Marangolo, M. Eddrief, J.-C. Boulliard, and V. H. Etgens, Phys. Rev. B **80**, 045403 (2009).
[18] C. Helman, V. Ferrari, and A. M. Llois, J. Phys. Conf. Ser. **568**, 042011 (2014).
[19] F. Ma, Z.-Y. Lu, and T. Xiang, Phys. Rev. B **78**, 224517 (2008).
[20] M. J. Calderón, B. Valenzuela, and E. Bascones, Phys. Rev. B **80**, 094531 (2009).
[21] M. Aichhorn, L. Pourovskii, V. Vildosola, M. Ferrero, O. Parcollet, T. Miyake, A. Georges, and S. Biermann, Phys. Rev. B **80**, 085101 (2009).
[22] I. Rungger and S. Sanvito, Phys. Rev. B **74**, 024429 (2006).
[23] G. Kresse and J. Furthmüller, Comput. Mater. Sci. **6**, 15 (1996).
[24] G. Kresse and D. Joubert, Phys. Rev. B **59**, 1758 (1999).
[25] J. P. Perdew, K. Burke, and M. Ernzerhof, Phys. Rev. Lett. **77**, 3865 (1996).
[26] H. Fjellvåg, A. Kjekshus, A. Andresen, and A. Zięba, J. Magn. Magn. Mater. **73**, 318 (1988).
[27] A. de Campos, D. L. Rocco, A. M. G. Carvalho, L. Caron, A. A. Coelho, S. Gama, L. M. da Silva, F. C. G. Gandra, A. O. dos Santos, L. P. Cardoso, P. J. von Ranke, and N. A. de Oliveira, Nat. Mater. **5**, 802 (2006).
[28] S. Graser, T. A. Maier, P. J. Hirschfeld, and D. J. Scalapino, New J. Phys. **11**, 025016 (2009).
[29] A. Saúl and G. Radtke, Phys. Rev. Lett. **106**, 177203 (2011).
[30] J. Goodenough, Phys. Rev. **100**, 564 (1955).